RTM for Inverse Elastic Scattering Problem

Shiqi Zhou ,
joint work with Zhiming Chen

Academy of Mathematics and System Science,
Chinese Academy of Science

2019.03.23 Wu Han

Content

Motivation

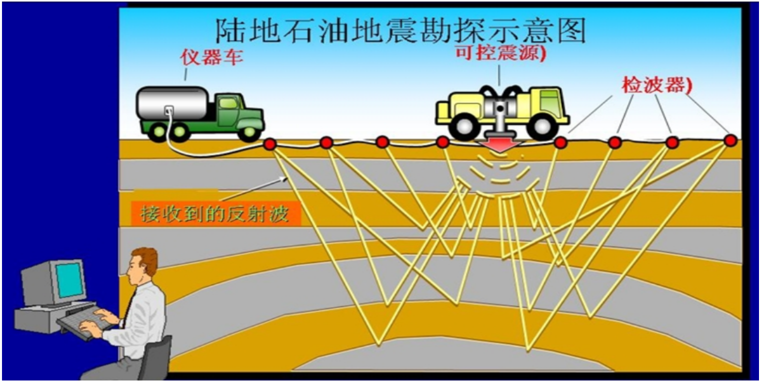

Figure: Find the support of the unknown obstacle from the knowledge of the scattered waves on a given surface.

Direct Scattering Problem in the Half Space

We consider elastic wave propagating in the half space with Neumann condition(Traction Free),

$$\nabla \cdot \sigma(u_q) + \rho\omega^2 u_q = -\delta_{x_s}(x)q \quad \text{in } \mathbb{R}^2_+ \backslash \bar{D}$$
$$u_q = 0 \quad \text{on } \Gamma_D \quad \text{and} \quad \sigma(u_q)\cdot e_2 = 0 \quad \text{on } \Gamma_0$$

together with the constitutive relation (Hookes law)

$$\sigma(u) = 2\mu\varepsilon(u) + \lambda \mathrm{div} u \mathbb{I}$$
$$\varepsilon(u) = \frac{1}{2}(\nabla u + (\nabla u)^T)$$

where ω is the circular frequency, $u(x) \in \mathbb{C}^2$ denotes the displacement fields and $\sigma(u)$ is the stress tensor. We also need to define the surface traction $T_x^n(\cdot)$ on the normal direction n,

$$T_x^n u(x) := \sigma \cdot n = 2\mu \frac{\partial u}{\partial n} + \lambda n \mathrm{div} u + \mu n \times \mathrm{curl} u$$

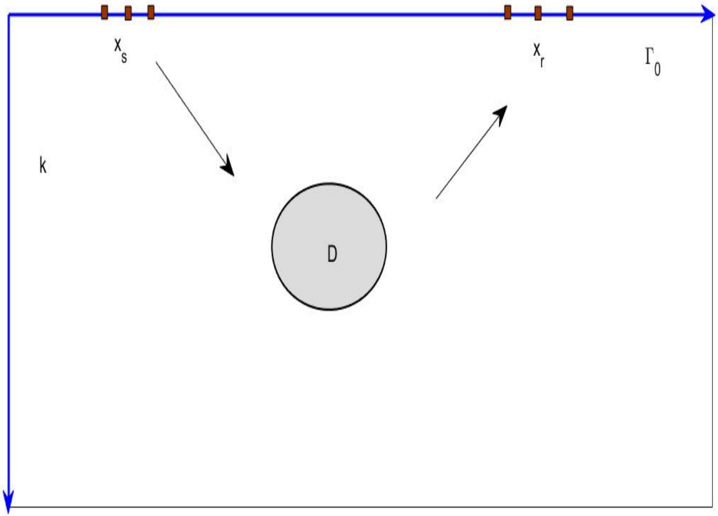
x_s
x_r
Γ_0
k
D

Green Tensor in the Half Space

Green Tensor in the half-space with Neumann boundary :

$$\Delta_e \mathbb{N}(x;y) + \omega^2 \mathbb{N}(x,y) = -\delta_y(x)\mathbb{I} \quad \text{in} \quad \mathbb{R}^2_+,$$
$$\sigma_x(\mathbb{N}(x,y))e_2 = 0 \qquad \text{on} \quad x_2 = 0$$

Green Tensor in the half-space with Dirichlet Boundary

$$\Delta_e \mathbb{D}(x,y) + \omega^2 \mathbb{D}(x,y) = -\delta_y(x)\mathbb{I} \quad \text{in} \quad \mathbb{R}^2_+,$$
$$\mathbb{D}(x,y) = 0 \qquad \text{on} \quad x_2 = 0$$

where $\delta_y(x)$ is the Dirac source at $y \in R^2_+$ and $N(x,y)$, $\mathbb{D}(x,y)$ are $\mathbb{C}^{2\times 2}$ matrixes.

Remark: we will assume that for $z \in \mathbb{C}$, $z^{1/2}$ is the analytic branch of $\sqrt{z}$ such that $\mathrm{Im}\,(z^{1/2}) \geq 0$.

Green Tensor in Frequency Domain after Fourier Transformation

$$\hat{\mathbb{N}}(\xi, x_2; y_2) = \hat{\mathbb{G}}(\xi, x_2; y_2) - \hat{\mathbb{G}}(\xi, x_2; -y_2) + \hat{\mathbb{N}}_c(\xi, x_2; y_2)$$

$$\hat{\mathbb{N}}_c(\xi, x_2; y_2) = \quad = \frac{\mathbf{i}}{\omega^2 \delta(\xi)} \Big\{ A(\xi) e^{\mathbf{i}\mu_s (x_2+y_2)} + B(\xi) e^{\mathbf{i}\mu_p (x_2+y_2)} + C(\xi) e^{\mathbf{i}\mu_s x_2 + \mu_p y_2} + D(\xi) e^{\mathbf{i}\mu_p x_2 + \mu_s y_2} \Big\}$$

where $\mathbb{G}(x, y)$ is the fundamental solution of elastic equation and

$$A(\xi) = \begin{pmatrix} \mu_s \beta^2 & -4\xi^3 \mu_s \mu_p \\ -\xi\beta^2 & 4\xi_4 \mu_p \end{pmatrix} \qquad B(\xi) = \begin{pmatrix} 4\xi^4 \mu_s & \xi\beta^2 \\ 4\xi^3 \mu_s \mu_p & \mu_p \beta^2 \end{pmatrix}$$

$$C(\xi) = \begin{pmatrix} 2\xi^2 \mu_s \beta & -2\xi \mu_s \mu_p \beta \\ -2\xi^3 \beta & 2\xi^2 \mu_p \beta \end{pmatrix} \quad D(\xi) = \begin{pmatrix} 2\xi^2 \mu_s \beta & 2\xi^3 \beta \\ 2\xi \mu_s \mu_p \beta & 2\xi^2 \mu_p \beta \end{pmatrix}$$

and $\mu_\alpha = (k_\alpha^2 - \xi^2)^{1/2}$, $\alpha \in \{s, p\}$, $\beta(\xi) = k_s^2 - 2\xi^2$, $\delta(\xi) = \beta^2 + 4\xi^2 \mu_s \mu_p$.

Dirichlet Green Tensor in Frequency Domain after Fourier Transformation

$$\hat{\mathbb{D}}(\xi, x_2; y_2) = \hat{\mathbb{G}}(\xi, x_2; y_2) - \hat{\mathbb{G}}(\xi, x_2; -y_2) + \hat{M}(\xi, x_2; y_2)$$

$$\begin{aligned} \hat{M}(\xi, x_2; y_2) \quad = \quad & \frac{\mathbf{i}}{\omega^2\gamma(\xi)}\Big\{ A(\xi)e^{\mathbf{i}\mu_s(x_2+y_2)} + B(\xi)e^{\mathbf{i}\mu_p(x_2+y_2)} \\ & -A(\xi)e^{\mathbf{i}\mu_s x_2 + \mu_p y_2} - B(\xi)e^{\mathbf{i}\mu_p x_2 + \mu_s y_2}\Big\} \end{aligned}$$

where

$$A(\xi) = \begin{pmatrix} \xi^2\mu_s & -\xi\mu_s\mu_p \\ -\xi^3 & \xi^2\mu_p \end{pmatrix} \qquad B(\xi) = \begin{pmatrix} \xi^2\mu_s & \xi^3 \\ \xi\mu_s\mu_p & \xi^2\mu_p \end{pmatrix}$$

and $\gamma(\xi) = \xi^2 + \mu_s\mu_p$.

Lemme 1

Let *Lamé* constant $\lambda, \mu \in \mathbb{R}^+$, then the Rayleigh equation $\delta(\xi) = 0$ has only two roots denoted by $\pm k_R$ in complex plane. Morever, $k_R > k_s > k_p$, $k_R \in \mathbb{R}$ and k_R is called Rayleigh wave number.

Using Cauchy integral theorem, we carry out:

Formula 1

$$\mathbb{N}(x, y) = \frac{1}{2\pi} \mathrm{P.V} \int_{\mathbb{R}} \hat{\mathbb{N}}(\xi, x_2; y_2) e^{\mathbf{i}(x_1 - y_1)\xi} d\xi - \frac{\mathbf{i}}{2} \frac{\mathbb{N}_\delta(-k_R)}{\delta'(-k_R)} e^{-\mathbf{i}(x_1 - y_1)k_R} + \frac{\mathbf{i}}{2} \frac{\mathbb{N}_\delta(k_R)}{\delta'(k_R)} e^{\mathbf{i}(x_1 - y_1)k_R}$$

where $\mathbb{N}_\delta(\xi) = \hat{\mathbb{N}}(\xi, x_2; y_2)\delta(\xi)$.

Lemma 2

Let *Lamé* constant $\lambda, \mu \in \mathbb{C}$ and $\mathrm{Im}\,(k_s) \geq 0, \mathrm{Im}\,(k_p) \geq 0$, then equation $\gamma(\xi) = 0$ has no root in complex plane.

Formula 2

Let $\mathbb{T}_D(x, y)$ denote the traction of $\mathbb{D}(x, y)$ in direction e_2 with respect to x such that $\mathbb{T}_D(x, y)e_i = \sigma_x(\mathbb{D}(x, y)e_i)e_2$.

$$\mathbb{T}_D(x, y) = \mathbb{T}(x, y) - \mathbb{T}(x, y') + \frac{1}{2\pi}\int_{\mathbb{R}} \hat{\mathbb{T}}_M(\xi, x_2; y_2)e^{\mathbf{i}(x_1 - y_1)\xi}d\xi$$

and

$$\hat{\mathbb{T}}_M(\xi, x_2; y_2) = \frac{\mu}{\omega^2\gamma(\xi)}\Big\{E(\xi)e^{\mathbf{i}\mu_s(x_2+y_2)} + F(\xi)e^{\mathbf{i}\mu_p(x_2+y_2)} - E(\xi)e^{\mathbf{i}\mu_s x_2 + \mu_p y_2} - F(\xi)e^{\mathbf{i}\mu_p x_2 + \mu_s y_2}\Big\}$$

where

$$E(\xi) = \begin{pmatrix} -\xi^2\beta & \xi\mu_p\beta \\ 2\xi^3\mu_s & -2\xi^2\mu_s\mu_p \end{pmatrix} \quad F(\xi) = \begin{pmatrix} -2\xi^2\mu_s\mu_p & -2\xi^3\mu_p \\ -\xi\mu_s\beta & -\xi^2\beta \end{pmatrix}$$

Asymptotic Behavior of Green Tensor

Theorem 1

Let $x \in \Gamma_0$, $y \in \mathbb{R}^2_+$ satisfy $|x_1 - y_1|/|x-y| \geq (1+\kappa)/2$ and $k_s y_2 \geq 1$. There exists a constant C depending only on κ such that

$$|\mathbb{N}(x,y)| + k_s^{-1}|\nabla_y \mathbb{N}(x,y)| \leq \frac{C}{\mu}\left(\frac{k_s y_2}{(k_s|x-y|)^{3/2}} + e^{-\sqrt{k_R^2 - k_s^2}\, y_2}\right).$$

Theorem 2

Let $x \in \Gamma_0$, $y \in \mathbb{R}^2_+$ satisfy $|x_1 - y_1|/|x-y| \geq (1+\kappa)/2$ and $k_s y_2 \geq 1$. There exists a constant C depending only on κ such that

$$|\mathbb{T}_D(x,y)| + k_s^{-1}|\nabla_y \mathbb{T}_D(x,y)| \leq C\frac{k_s^2 y_2}{(k_s|x-y|)^{3/2}}.$$

Inverse Scarttering Problem

$$\begin{cases} \nabla \cdot \sigma(u_q) + \rho\omega^2 u_q = -\delta_{x_s}(x)q & in \quad \mathbb{R}^2_+ \backslash \bar{D} \\ u_q = 0 & on \quad \Gamma_D \\ \sigma(u_q) \cdot e_2 = 0 & on \quad \Gamma_0 \end{cases}$$

satisfies the generalized radiation condition

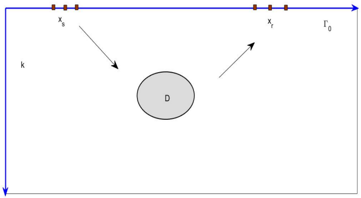

Direct Problem

To determine the scattering wave field $u^s(x, x_s) = u(x, x_s) - u^i(x, x_s)$ from the given incident field $u^i(x, x_s) = \mathbb{N}(x, x_s)$, the differential equation governing the wave motion and the information of obstacle.

Inverse problem

To determine the location, size, sharp of the obstacle by the measured field $u^s(x, x_s)$ on x_r

Direct Scattering Problem

We recall the classical argument of limiting absorption principle to define the scattering solution for the exterior elastic scattering problem in the half space:

$$\Delta_e u + \omega^2 u = 0 \quad \text{in } \mathbb{R}^2_+ \backslash \bar{D}, \tag{1}$$

$$u = g \quad \text{on } \Gamma_D, \qquad \sigma(u)e_2 = 0 \quad \text{on } \Gamma_0, \tag{2}$$

where $g \in H^{1/2}(\Gamma_D)$. Let $\varepsilon > 0$ and u_ε be the solution of the problem

$$\Delta_e u_\varepsilon + [\omega(1 + \mathbf{i}\varepsilon)]^2 u_\varepsilon = 0 \quad \text{in } \mathbb{R}^2_+ \backslash \bar{D}, \tag{3}$$

$$u_\varepsilon = g \quad \text{on } \Gamma_D, \qquad \sigma(u_\varepsilon)e_2 = 0 \quad \text{on } \Gamma_0. \tag{4}$$

Theorem 3

Let $g \in H^{1/2}(\Gamma_D)$. The half-space elastic scattering problem (1)-(2) admits a unique solution $u \in H^1_{\text{loc}}(\mathbb{R}^2_+ \backslash \bar{D})$. Moreover, for any bounded open set $\mathcal{O} \subset \mathbb{R}^2_+ \backslash \bar{D}$ there exists a constant $C > 0$ such that $\|u\|_{H^1(\mathcal{O})} \leq C\|g\|_{H^{1/2}(\Gamma_D)}$.

Algorithms of inverse obstacle problem

Direct Imaging Method

- Linear Sample MethodFactorization methodPoint source method
- MUltiple SIgnal Classification
- Prestack depth migrationReverse Time Migration

Feature

Fast computationDifficult mathematics analysis

Iterative Method

- Differential semblance optimization
- Full waveform inversion
- Recursive linearization algorithm

Feature

Need prior information, Difficult to convergence, Provide quantitative information

Reverse Time Migration

- Do not require any priori information of the physical properties of the obstacle such as penetrable or non-penetrable, and for non-penetrable obstacles, the type of boundary conditions on the boundary of the obstacle.
- The previous analysis of the migration method is usually based on the high frequency assumption so that the geometric optics approximation can be used.

Reverse Time Migration: Mathematics Framework

Acoustic, electromagnetic, elastic wave in the Full space

1. Chen J, Chen Z, Huang G. *Reverse time migration for extended obstacles: acoustic waves [J]*. Inverse Problems. 2013, 29(8):645-648
2. Chen J, Chen Z, Huang G. *Reverse time migration for extended obstacles: Electromagnetic waves[J]*. Scientia Sinica, 2015, 29(8):085005.
3. Chen Z, Huang G. *Reverse time migration for extended obstacles: Elastic waves (in Chinese)[J]*. Science China Mathematics, 2015, 45(8):1103-1114.

Planar acoustic waveguide

1. Chen Z M, Huang G H. *Reverse time migration for reconstructing extended obstacles in planar acoustic waveguides[J]*. Science China Mathematics, 2015, 58(9):1811-1834.

Acoustic in the Half space

1. Chen Z, Huang G. *Reverse time migration for reconstructing extended obstacles in the half space[J]*. Inverse Problems, 2015, 31(5):055007 (19pp).

Phaseless Algorithm

1. Chen Z, Huang G. *Phaseless Imaging by Reverse Time Migration: Acoustic Waves[J]*. Numerical Mathematics Theory Methods and Applications, 2017, 10(1):1-21.

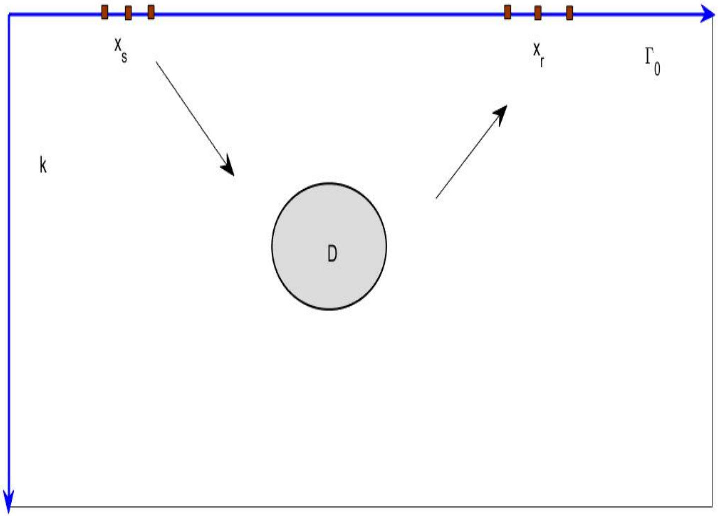
x_s
x_r
Γ_0
k
D

RTM Algorithm

Given the data $u_k^s(x_r, x_s)$, $k = 1, 2$ which is the measurement of the scattered field at x_r when the source is emitted at x_s along the polarized direction e_k, $s = 1, \dots, N_s$ and $r = 1, \dots, N_r$

1° Back-propagation: Compute $v_q(x, x_s)$ as the scattering solution of the following half-space elastic scattering problem:

$$\Delta_e v_q(x, x_s) + \omega^2 v_q(x, x_s) = 0 \quad \text{in } \mathbb{R}_+^2,$$

$$v_q(x, x_s) = \frac{|\Gamma_0^d|}{N_r} \sum_{r=1}^{N_r} \overline{u_q^s(x_r, x_s)} \delta_{x_r}(x) \quad \text{on } \Gamma_0.$$

2° Cross-correlation: For each $z \in \Omega$, compute the imaging function

$$I_d(z) = \operatorname{Im} \sum_{q=e_1,e_2} \left\{ \frac{|\Gamma_0^d|}{N_s} \sum_{s=1}^{N_s} u_q^i(z, x_s) \cdot v_q(z, x_s) \right\}. \tag{5}$$

RTM Algorithm

By the integral representation formula, we know that

$$v_q(x,x_s)\cdot e_j = \frac{|\Gamma_0^d|}{N_r}\sum_{r=1}^{N_r}\mathbb{T}_D(x_r,x)e_j\cdot\overline{u_q^s(x_r,x_s)},$$

which yields

$$I_d(z) = \mathrm{Im}\sum_{q=e_1,e_2}\left\{\frac{|\Gamma_0^d|^2}{N_sN_r}\sum_{s=1}^{N_s}\sum_{r=1}^{N_r}[\mathbb{T}_D(x_s,z)^Tq]\cdot[\mathbb{T}_D(x_r,z)^T\overline{u_q^s(x_r,x_s)}]\right\}.$$

This is the formula will be used in our numerical examples in section 6. By letting $N_s,N_r\to\infty$, we know that (5) can be viewed as an approximation of the following continuous integral:

$$\hat{I}_d(z) = \mathrm{Im}\sum_{q=e_1,e_2}\int_{\Gamma_0^d}\int_{\Gamma_0^d}[\mathbb{T}_D(x_s,z)^Tq]\cdot[\mathbb{T}_D(x_r,z)^T\overline{u_q^s(x_r,x_s)}]\,ds(x_r)ds(x_s).$$

Point Spread Function

The point spread function measures the resolution to find a point source. Given the $\mathbb{N}(x,y)$ on $\Gamma_0^d = \{(x_1,x_2)^T \in \Gamma_0,\ x_1 \in (-d,d)\}$ with the source $y \in \mathbb{R}^2_+$, we define the PSF as the back-propagated field $\mathbb{J}_d(x,y)$.

$$\begin{aligned} &\Delta_e \mathbb{J}_d(x,y) + \omega^2 \mathbb{J}_d(x,y) = 0 \quad \text{in} \quad \mathbb{R}^2_+, \\ &\mathbb{J}_d(x,y) = \overline{\mathbb{N}(x,y)}\chi_{(-d,d)} \qquad \text{on} \quad \Gamma_0 \end{aligned}$$

By integral representation

$$\begin{aligned} \mathbb{J}_d^{ij}(z,y): &= e_i \cdot \mathbb{J}_d(z,y)e_j \\ &= \int_{\Gamma_0^d} \sigma_x(\mathbb{D}(x,z)e_i)e_2 \cdot \overline{\mathbb{N}(x,y)}e_j ds(x) \\ &= \int_{-d}^{d} \sigma_x(\mathbb{D}(x_1,0;z_1,z_2)e_i)e_2 \cdot \overline{\mathbb{N}(x_1,0;y_1,y_2)}e_j dx_1 \end{aligned}$$

Numerical test: PSF

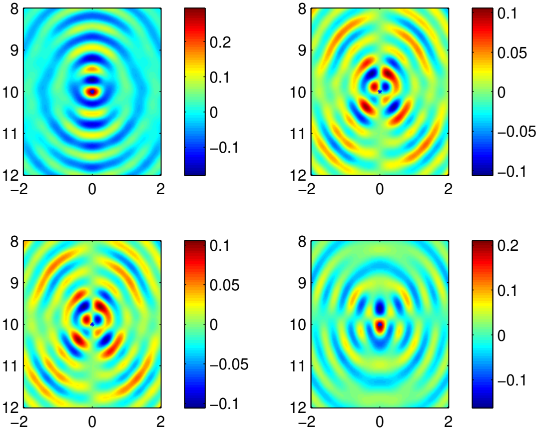

Figure: The figures on the diagonal line show that psf have peaks on the point x=y

Analysis of PSF

Hypothesis

We assume the obstacle $D \subset \Omega$ and there exist constants $0 < c_1 < 1, c_2 > 0, c_3 > 0$ such that

$$h < d, \quad |x_1| \le c_1 d, \quad |x_1 - y_1| \le c_2 h, \quad |x_2| \le c_3 h \quad \forall x, y \in \Omega$$

Lemma 3

Let $k_s h > 1$. For any $z, y \in \Omega$, PSF can be reprsented by $J_d(z,y) = \mathbb{F}(z,y) + \mathbb{R}(z,y)$ and it satisfy that

$$|\mathbb{R}_{ij}(z,y)| + k_s^{-1}|\nabla_y \mathbb{R}_{ij}(z,y)| \le \frac{C}{\mu}\left(\frac{1}{(k_s h)^{\frac{1}{2n^*}}} + k_s h e^{-k_s h\sqrt{\kappa_R^2 - 1}}\right) + \frac{C}{\mu}\left(\left(\frac{h}{d}\right)^2 + \frac{(k_s h)^{1/2}}{e^{k_s h\sqrt{\kappa_R^2 - 1}}}\left(\frac{h}{d}\right)^{1/2}\right)$$

uniformly for $z, y \in \Omega$. Here $\kappa_R := k_R / k_s$ and the constant C may dependent on $k_s d_D$ and $\kappa := k_p / k_s$, but is independent of k_s, k_p, h, d_D.

Main Term of PSF

Based on the above argument, we know that $\mathbb{R}(z,y)$ becomes small when z,y move away from Γ_0 and $d \gg h$. Our goal is to show $\mathbb{F}(z,y)$ has the similar decay to the elastic fundamental solution $\operatorname{Im}\Phi(z,y)$ as $|z-y| \to \infty$.

Theorem 4

For any $z, y \in \mathbb{R}^2_+$, when $z = y$

$$|\operatorname{Im}\mathbb{F}_{ii}(z,y)| \geq \frac{1}{4(\lambda+2\mu)}\ ,\ i=1,2$$
$$\operatorname{Im}\mathbb{F}_{12}(z,y) = \operatorname{Im}\mathbb{F}_{21}(z,y) = 0$$

and for $z \neq y$

$$|\mathbb{F}_{ij}(z,y)| \quad \leq \frac{C}{\mu}[(k_s|z-y|)^{-1/2}) + (k_s|z-y|^{-1})]$$

where constant C is only dependent on $\kappa := k_p/k_s$.

Now, We turn to study the resolution of the function $\hat{I}_d(z)$. To do this, we first show the difference between the half space scattering solution and the full space scattered solution is small if the scatterer is far away from the boundary Γ_0.

Theorem 5

Let $g \in H^{1/2}(\Gamma_D)$ and $\mathbf{u}_1, \mathbf{u}_2$ be the scattering solution of following problems:

$$\begin{aligned} \Delta_e \mathbf{u}_1 + \omega^2 \mathbf{u}_1 = 0 \qquad & \text{in } \mathbb{R}^2_+ \backslash \bar{D} \\ \mathbf{u}_1 = g \quad & \text{on } \Gamma_D \\ \sigma(\mathbf{u}_1) e_2 = 0 \quad & \text{on } \;\Gamma_0 \end{aligned}$$

and

$$\begin{aligned} \Delta_e \mathbf{u}_2 + \omega^2 \mathbf{u}_2 = 0 \qquad & \text{in } \mathbb{R}^2 \backslash \bar{D} \\ \mathbf{u}_2 = g \quad & \text{on } \Gamma_D \end{aligned}$$

Then there exits a constant C independent of k_s, k_p, such that

$$\|\sigma_x(\mathbf{u}_1 - \mathbf{u}_2)\nu\|_{H^{-1/2}(\Gamma_D)} \le \frac{C}{\mu}(1 + \|T_f\|)(1 + \|T_h\|)(1 + k_s d_D)^2 \epsilon_1(k_s h) \|g\|_{H^{1/2}(\Gamma_D)}$$

Resolution Analysis

Theorem 6

For any $z \in \Omega$, let $\mathbb{U}(z,x) \in \mathbb{C}^{2\times 2}$ such that $\mathbb{U}(z,x)e_j$, $j = 1, 2$, is the scattering solution of the problem:

$$\Delta_e[\mathbb{U}(z,x)e_j] + \omega^2[\mathbb{U}(z,x)e_j] = 0 \ \text{ in } \mathbb{R}^2\backslash\bar{D}, \qquad \mathbb{U}(z,x)e_j = -\overline{\mathbb{F}(z,x)}e_j \ \text{ on } \Gamma_D.$$

Then, we have

$$\hat{I}_d(z) = \mathrm{Im}\sum_{j=1}^{2}\int_{\Gamma_D}[\sigma(\mathbb{U}(z,x)e_j + \overline{\mathbb{F}(z,x)}e_j)\nu]\cdot[\overline{\mathbb{F}(z,x)}e_j]ds(x) + R_d(z), \tag{6}$$

where $|R_d(z)| \leq C\mu^{-2}(1+\|T_1\|)(1+\|T_2\|)(1+k_s d_D)^3\left[\left(\frac{h}{d}\right)^2 + (k_s h)^{-1/4}\right]$ for some constant C depending only on κ but independent of k_s, k_p, h, d, d_D.

Numerical Test: Different Boundary Condition

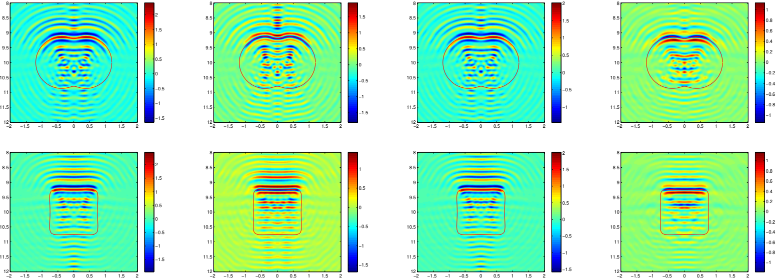

Figure: Example 1: From left to right: imaging results of a Dirichlet, a Neumann, a Robin bounday with impedance $\eta(x) = 1$, and a penetrable obstacle with diffractive index $n(x) = 0.25$

Numerical Test: Different Sharp

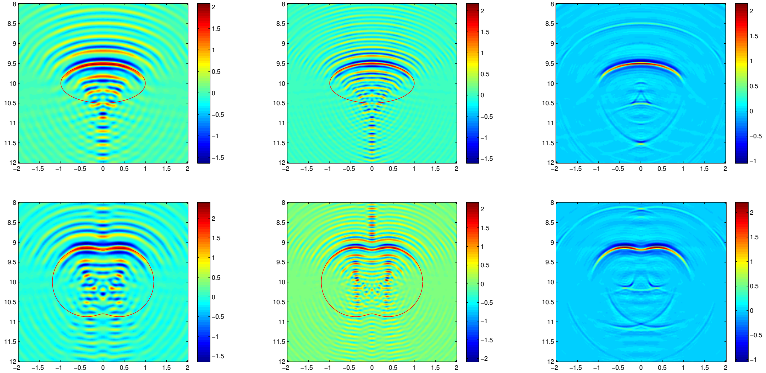

Figure: Example 2: Imaging results of clamped obstacles with different shapes from top to below. The left row is imaged with single frequency data where $\omega = 3\pi$, The middle row is imaged with single frequency data where $\omega = 5\pi$ and The left row is imaged with multi frequency data

Numerical Test: Different Sharp

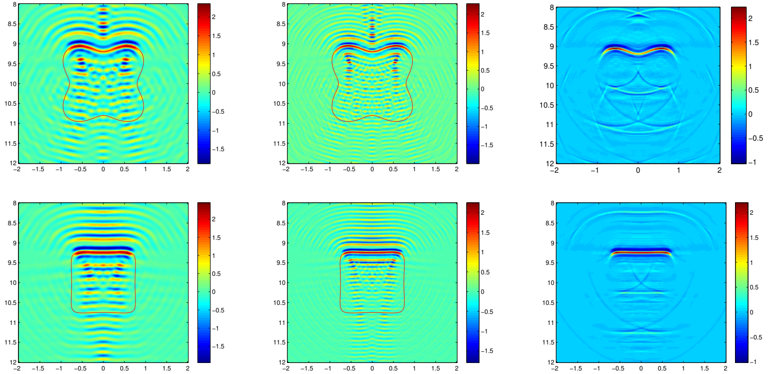

Figure: Example 3: Imaging results of clamped obstacles with different shapes from top to below. The left row is imaged with single frequency data where $\omega = 3\pi$, The middle row is imaged with single frequency data where $\omega = 5\pi$ and The left row is imaged with multi frequency data

Numerical Test: Two Obstacles

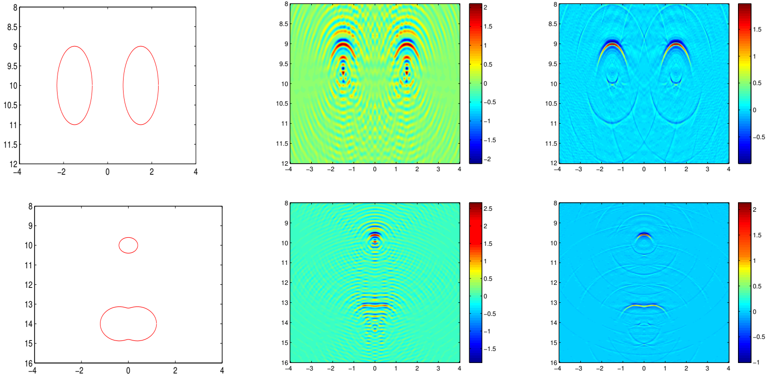

Figure: Example 4:From left to right, true obstacle model with two circles. the imaging result with single frequency data where $\omega = 3\pi$, the imaging result with multiple frequency data.

Numerical Test: additive Gaussian noise

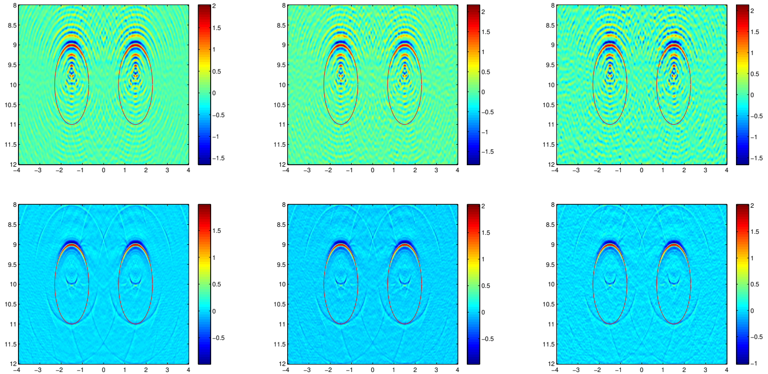

Figure: Example 5: Imaging results of a clamped obstacle with noise levels $\mu = 0.2; 0.3; 0.4$ (from left to right). The top row is imaged with single frequency data where $\omega = 4\pi$, and the bottom row is imaged with multi-frequency data.

Physical interpretation: high frequence

Let y(s) be the arc length parametrization of the boundry Γ_D and $y_{\pm}(\eta_\theta) = y(s_{\pm})$ be the pionts such that $\nu(y(s_{\pm})) = \pm\eta_\theta$ and $\eta(y)$ be Gauss curvature. In the case of $\omega \gg 1$, by stationary phase theorem and Kirchhoff approximation, the imaging function for the clamped obstacle is

$$\begin{aligned}\hat{I}_d(z) &\approx \sqrt{8\pi k_p}\mathrm{Im}\,\mathbf{tr}\int_0^\pi ((\lambda+2\mu)A_p(\theta)\eta_\theta e^{\mathbf{i}k_p(y_-(\eta_\theta)-z)\cdot\eta_\theta-\mathbf{i}\frac{\pi}{4}})^T\frac{\overline{F(z,y_-(\eta_\theta))}}{\sqrt{\vartheta(y_-(\eta_\theta))}}d\theta \\ &+ \sqrt{8\pi k_s}\mathrm{Im}\,\mathbf{tr}\int_0^\pi (\mu A_s(\theta)\eta_\theta^\perp e^{\mathbf{i}k_s(y_-(\eta_\theta)-z)\cdot\eta_\theta-\mathbf{i}\frac{\pi}{4}})^T\frac{\overline{F(z,y_-(\eta_\theta))}}{\sqrt{\vartheta(y_-(\eta_\theta))}}d\theta\end{aligned}$$

Now for z in the part of Γ_D which is back to Γ_0, ie $\nu(z)\cdot\eta_\theta > 0$ for any $\theta\in[0,\pi]$, we know that z and $y_-(\eta_\theta)$ are far away and thus $\hat{I}_d(z)\approx 0$. By above formula , we can explain that one cannot image the back part of the obstacle with only the data collected on Γ_0. This confirmed in our numerical examples.

Conclusion

- New form and asymptotic analysis of Green tensor in the half space..
- Regularity estimate of direction elastic wave equation in the Half-space.
- Mathematics analysis of point spread function.
- Resolution analysis of Reverse Time Migration without any geometric optics approximation .
- Scattered wave data simulation and numerical test of RTM.

Thank you !